The Astrophysical Journal, 719:950–957, 2010 August 10 doi:10.1088/0004-637X/719/1/950

THE ORTHOGONAL FITTING PROCEDURE FOR DETERMINATION OF THE EMPIRICAL Σ–D RELATIONS FOR SUPERNOVA REMNANTS: APPLICATION TO STARBURST GALAXY M82

D. Urošević[1,2], B. Vukotić[3], B. Arbutina[1], and M. Sarevska[4]
[1] Department of Astronomy, Faculty of Mathematics, University of Belgrade, Studentski trg 16, 11000 Belgrade, Serbia; dejanu@math.rs, arbo@math.rs
[2] Isaac Newton Institute of Chile, Yugoslavia Branch
[3] Astronomical Observatory, Volgina 7, 11060 Belgrade 38, Serbia; bvukotic@aob.rs
[4] University of Niš, Serbia
Received 2010 March 15; accepted 2010 June 23; published 2010 July 23

ABSTRACT

The radio surface brightness-to-diameter (Σ–D) relation for supernova remnants (SNRs) in the starburst galaxy M82 is analyzed in a statistically more robust manner than in the previous studies that mainly discussed sample quality and related selection effects. The statistics of data fits in the $\log\Sigma$–$\log D$ plane are analyzed by using vertical (standard) and orthogonal regressions. As the parameter values of D–Σ and Σ–D fits are invariant within the estimated uncertainties for orthogonal regressions, slopes of the empirical Σ–D relations should be determined by using the orthogonal regression fitting procedure. Thus obtained Σ–D relations for samples which are not under severe influence of the selection effects could be used for estimating SNR distances. Using the orthogonal regression fitting procedure, the Σ–D slope $\beta \approx 3.9$ is obtained for the sample of 31 SNRs in M82. The results of implemented Monte Carlo simulations show that the sensitivity selection effect does not significantly influence the slope of the M82 relation. This relation could be used for estimating distances to SNRs that evolve in a denser interstellar environment, with number density up to 1000 particles per cm^3.

Key words: galaxies: individual (M82) – ISM: supernova remnants – methods: statistical – radio continuum: ISM

1. INTRODUCTION

The relation between surface brightness (Σ) and diameter (D) for supernova remnants (SNRs)—known as the Σ–D relation—is a standard way for investigating the radio brightness evolution of these sources. In the vast majority of situations, it is not feasible to observe the detailed evolution of individual SNRs over very long periods of time. However, by studying the properties of samples of SNRs, which cover a range of different ages but are assumed to follow similar evolutionary paths, it is possible to analyze their statistical properties and evolution. Understanding the statistical and evolutionary properties of SNR samples and particularly using well-defined samples to determine the Σ–D relation also has an important role in providing a method of distance determination for individual SNRs. This is particularly relevant for Galactic SNRs, of which more than 200 have unknown or ill-determined distance measures (see, for example, Green 2009).

In a single external galaxy, all SNRs in the sample are at essentially the same distance. This makes the extragalactic samples of better quality when compared to Galactic ones, because the problems stemming from inaccurate knowledge of distances are eliminated. Additionally, Malmquist bias[5] severely acts in the Galactic samples making them incomplete. An extragalactic sample is not influenced by the Malmquist bias. On the other hand, the best radio instruments at this moment can provide detection of brighter SNRs only in the nearby galaxies. Such a limited survey sensitivity results in a selection effect that significantly reduces the number of detected objects within a relatively distant extragalactic system (approximately up to 15 Mpc; see Urošević et al. 2005, hereafter Paper I; Chomiuk & Wilcots 2009).

This paper presents a fitting procedure that can result, if reliable samples are used, in Σ–D relations that are more useful in terms of distance estimation. The usual form of the relation is

$$\Sigma = A D^{-\beta}, \tag{1}$$

where parameter A and slope β are obtained by fitting the observational data for a sample of SNRs.

The two initial empirical Σ–D relations were derived by Poveda & Woltjer (1968) and Milne (1970). During the 1970s and early 1980s, a number of detailed analyses of Galactic relations were presented (e.g., Clark & Caswell 1976; Milne 1979). More critical analysis started with the work of Green (1984). A Galactic Σ–D relation that is still quite frequently used was derived by Case & Bhattacharya (1998). A brief review of Galactic and extragalactic relations was presented by Urošević (2002). The updated Galactic Σ–D relations were derived by Guseinov et al. (2003) and Xu et al.(2005).

The best sample for the Σ–D analysis consists of compact SNRs from starburst galaxy M82 (see Arbutina et al. 2004; Paper I). The analyzed sample (21 SNRs) was taken from Huang et al. (1994) and McDonald et al. (2002). This sample is different than other Galactic and extragalactic samples because it has the steepest Σ–D slope (see Paper I) and shows a relatively high degree of L–D correlation (for more on the L–D correlation and trivial Σ–D relation concept, see Arbutina et al. 2004). Furthermore, unlike other samples, it consists of a relatively high number of very small and very bright SNRs (Paper I; Fenech et al. 2008, hereafter F08). It is important to note that in an extragalactic sample all the SNRs are essentially at the same distance, wherefore a uniformly sensitive survey has a uniform sensitivity in luminosity or surface brightness for all SNRs within the sample. The survey sensitivity selection effect has a weaker influence on the M82 Σ–D slope than on the slopes derived for other nearby galaxies because M82 SNRs are of relatively high brightness. This is shown in Paper I on Monte Carlo generated artificial extragalactic samples; after generating the sample, a sensitivity cutoff is applied selecting only the points above the survey sensitivity line. The apparent

[5] The volume selection effect—intrinsically bright objects are favored in any flux-limited survey because they are sampled from a larger spatial volume.

Table 1
Summary Characteristics of the Selected Samples (the Number of Sources in Sample and Range of Relevant Quantities)

Relevant Quantities	S1	S2
N^a	31	10
S^b (mJy)	[0.099, 19.435]	[0.72, 39.01]
L(J s^{-1} Hz^{-1})	[1.21×10^{17}, 2.38×10^{19}]	[8.82×10^{17}, 4.78×10^{19}]
D(pc)	[0.64, 6.2]	[0.205, 2.25]
Σ(W m^{-2} Hz^{-1} sr^{-1})	[9.24×10^{-19}, 4.16×10^{-15}]	(6.42×10^{-17}, 1.22×10^{-13})

Notes. The adopted M82 distance is 3.2 Mpc (F08) which provides a linear size equivalent to 1 mas ≡ 0.0155 pc (as used in F08).
[a] The number of sources in the sample.
[b] Integrated flux density.

(after selection) and true (before selection) fitted slopes of the simulated samples are then compared with the slopes fitted to the real data.

In this paper, we use the new observations of compact SNRs in M82 by F08. From F08, we extract a data set that consists of 31 SNRs and fit Σ–D regression for both orthogonal and vertical offsets. Additionally, Monte Carlo simulations are performed to illustrate the selection effect of survey sensitivity on the fitted Σ–D slopes for the M82 sample (the simulation algorithm is explained in more detail in Section 5).

2. THE M82 DATA SAMPLE

All data analyzed herein are collected from F08. The central kpc of M82 was mapped at 5 GHz using the Multi-Element Radio Linked Interferometer Network (MERLIN). The largest detectable angular size with this array at 5 GHz is ∼1.2 arcsec (18.5 pc at the distance of M82). Fenech et al. present new MERLIN observations made in 2002 along with observations made 10 years earlier which were previously published by Muxlow et al. (1994). Depending on particular image parameters, the angular resolution in 1992 and 2002 data varies in the range 35–50 mas (0.54–0.78 pc), but all sources were resolved with a 35 mas beam (F08). Also, the rms noise in the 2002 data images varies in the range 17–24 μJy beam^{-1} and 46–60 μJy beam^{-1} for the 1992 data images (F08).

The sources from the 2002 observation are listed in Table 2 of F08. Out of 55 sources there are 36 SNRs. For the purpose of this paper, we have excluded five SNRs with the largest angular size diameter estimates (sources with peak flux $\lesssim$0.1 mJy beam^{-1}). Inspection of Figure 3 in F08 shows that these five sources are mostly of non-compact structure with only the brightest parts above the sample sensitivity limit (0.085 mJy beam^{-1}). Consequently, these sources are easily confused with noise and the diameters of their faint extended structures cannot be accurately estimated. This left us with the 31 SNRs data set, referred to as S1 further in the text. While all the data in S1 have associated integrated flux density errors, only seven points have associated diameter errors. To calculate the error in Σ, we need both flux density errors and diameter errors. Table 3 from F08 presents flux densities, diameters, and associated errors for 10 SNRs observed with MERLIN in 1992 (not necessarily listed in Table 2 of F08). We used these 1992 measurements of flux densities, diameters, and associated errors; this sample is further referred to as S2. For elliptical sources, we calculated the mean geometric diameter (for both S1 and S2). The fits of non-weighted vertical and orthogonal offsets for S1, and non-weighted and weighted vertical and orthogonal offsets for S2, are presented in the following section. In Table 1, we present the range of relevant quantities for samples S1 and S2.

3. FITTING

The standard fitting procedure in the Σ–D plane based on the vertical (parallel to the y-axis) χ^2 regression has been used for the calibration of empirical Σ–D relations. Recently, Bandiera & Petruk (2010) have used a different method: regression analysis with two independent variables—diameter D and the density of environment n_0. In this paper, we stay with one independent variable D (or Σ) but change the fitting procedure from vertical to orthogonal offsets. Dependence on n_0 is important for Σ–D analysis. M82 SNRs evolve in a denser environment (Chevalier & Fransson 2001; Arbutina & Urošević 2005), but variation in the ambient density certainly exists. This is consistent with observations of structural evolution and the wide range of expansion velocities of individual SNRs in M82 (e.g., F08; Pedlar et al. 1999; McDonald et al. 2001; Beswick et al. 2006; Fenech et al. 2010). Variation in expansion velocities is probably constrained by the differences in ambient density. This variation in density, if it is assumed that the SNRs are evolving along similar evolutionary tracks, probably does provide one of the key reasons for the moderately large scatter in the plotted Σ–D correlation.

For a description of the radio surface brightness evolution of an SNR, we should investigate Σ–D correlation, while for the distance determination of SNRs we need the D–Σ correlation (see Green 2009). The starting point of our analysis is the requirement that the D–Σ and Σ–D fit parameter values are invariant within the estimated uncertainties. This can be achieved with the orthogonal regression fitting procedure. Here, we use both types of fitting, standard (vertical) and orthogonal, and compare the results.

Data fitting is performed numerically. We search for the minimum of the χ^2 function using the simplex algorithm (O'Neil 1971). The fit parameter values and their errors, presented in Tables 2–4, are the mean values and associated standard deviations after 10,000 bootstrap data re-samplings for each fit. When fitting with data errors, the vertical offsets are weighted with $\sigma_{y_i}^2$, while orthogonal offsets χ^2 are calculated as $\frac{(y_i - A - \beta x_i)^2}{\sigma_{y_i}^2 + (\sigma_{x_i}\beta)^2}$.

4. ANALYSIS OF FIT STATISTICS

At first glance, inspection of Figures 1 and 2 and the Tables leads to the conclusion that resulting fit parameter values are significantly influenced by the type of fitting procedure. The Σ–D slopes are obviously steeper for orthogonal offsets (Figures 1 and 2; Table 2). The approximately "trivial" Σ–D slope ($\beta \approx 2.4$) is transformed into a very steep slope ≈3.9 for the S1 sample of 31 SNRs (Table 2). Also, for the poorer sample with respect to the number of objects (10 S2 SNRs), steeper

Table 2
The Σ–D Relation

Fit	log A	Δ log A	β	$\Delta\beta$	Q	WSSR/ndof	$\sqrt{\text{WSSR/ndof}}$
The sample of 10 SNRs from Table 3 in F08, $r = -0.924164$, $r^2 = 85.407974\%$.							
Ver. os.	−15.2842	1.48035e−01	3.00753	0.43692	9.92070e−01	1.92172e−01	4.38374e−01
Ver. os. w.	−14.9625	1.99015e−01	2.88255	0.41673	0.00000e+00	2.08336e+02	1.44338e+01
Ort. os.	−15.2874	1.56158e−01	3.60747	0.52914	9.99999e−01	1.62385e−02	1.27430e−01
Ort. os. w.	−14.9921	1.82236e−01	3.08412	0.47155	1.07173e−201	1.19871e+02	1.09485e+01
The sample of 31 SNRs from Table 2 in F08, $r = -0.782763$, $r^2 = 61.271836\%$.							
Ver. os.	−15.7409	2.01064e−01	2.41576	0.43166	9.99967e−01	2.71169e−01	5.20739e−01
Ort. os.	−15.2535	1.87001e−01	3.85631	0.43339	1.00000e+00	2.58510e−02	1.60783e−01

Table 3
The $L = BD^{-\delta}$ Relation

Fit	log B	Δ log B	δ	$\Delta\delta$	Q	WSSR/ndof	$\sqrt{\text{WSSR/ndof}}$
The sample of 10 SNRs from Table 3 in F08, $r = -0.641483$, $r^2 = 41.150074\%$							
Ver. os.	18.6909	1.40852e−01	1.01038	0.43436	9.92093e−01	1.92008e−01	4.38187e−01
Ver. os. w.	19.0008	2.31966e−01	0.80511	0.57985	0.00000e+00	1.62263e+03	4.02818e+01
Ort. os.	18.6929	3.11494e−01	2.21533	0.95097	9.99888e−01	5.97075e−02	2.44351e−01
Ort. os. w.	18.9292	2.20137e−01	1.35415	0.82877	0.00000e+00	8.40500e+02	2.89914e+01
The sample of 31 SNRs from Table 2 in F08, $r = -0.236428$, $r^2 = 5.589839\%$							
Ver. offst.	18.2409	2.01469e−01	0.43333	0.43048	9.99971e−01	2.68603e−01	5.18269e−01
Ort. offst.	19.1334	7.52688e−01	2.96520	1.40621	1.00000e+00	7.25849e−02	2.69416e−01

Table 4
The D–Σ Relation

Fit	Coefficient	ΔCoefficient	$1/\beta$	$\Delta(1/\beta)$	Q	WSSR/ndof	$\sqrt{\text{WSSR/ndof}}$
The sample of 10 SNRs from Table 3 in F08, $r = -0.924164$, $r^2 = 85.407974\%$							
Ver. os.	−4.26141	5.54597e−01	0.27896	0.03736	9.99999e−01	1.74798e−02	1.32211e−01
Ver. os. w.	−4.66426e	6.73978e−01	0.31067	0.04486	0.00000e+00	2.80880e+02	1.67595e+01
Ort. os.	−4.32109e	5.48758e−01	0.28290	0.03697	9.99999e−01	1.61987e−02	1.27274e−01
Ort. os. w.	−4.93663	6.22588e−01	0.32945	0.04178	2.32472e−200	1.19097e+02	1.09131e+01
The sample of 31 SNRs from Table 2 in F08, $r = -0.782763$, $r^2 = 61.271836\%$.							
Ver. os.	−3.83090	4.62411e−01	0.25182	0.02793	1.00000e+00	2.75240e−02	1.65904e−01
Ort. os.	−4.00880	5.02672e−01	0.26253	0.03021	1.00000e+00	2.58590e−02	1.60807e−01

slopes are obtained, but the differences are not so huge as in the case of the larger sample (see Table 2). On the other hand, D–Σ slopes are approximately the same in both fitting procedures (see Table 4). This is due to a rather small span of diameters (1 order of magnitude) in comparison to the span of surface brightnesses (4 orders of magnitude). This leads to flatter slopes which results in similar lengths of vertical and orthogonal offsets giving similar fit parameters.

For the proper Σ–D analysis, the L–D correlation should be checked. If the L–D correlation does not exist, the trivial $\Sigma \propto D^{-2}$ form should not be used (Arbutina et al. 2004). The statistics of L–D correlations for both M82 samples are rather poor. For the S2 sample, this is because of the relatively low coefficient of correlation and a small number of objects in the sample, while for the S1 sample, it is because of a very low coefficient of correlation. The coefficient of correlation r is calculated using the following equation:

$$r = \frac{\sum_i (x_i - \overline{x})(y_i - \overline{y})}{\sqrt{\sum_i (x_i - \overline{x})^2}\sqrt{\sum_i (y_i - \overline{y})^2}}. \quad (2)$$

Finally, based on the poor statistical results of the L–D fits (Table 3), it can be concluded that both extracted samples show a high degree of scattering.

5. MONTE CARLO SIMULATIONS

We performed a set of Monte Carlo simulations to estimate the influence of the survey sensitivity selection effect on the Σ–D slope for the M82 sample (31 SNRs). In both fitting procedures (vertical and orthogonal), we used the algorithm described below.

5.1. Vertical Offsets

Monte Carlo simulations are similar to those described in Paper I. First, we determined the empirical log Σ standard deviation from the best-fit line, assuming log D as the independent variable. We then selected an interval in log D between 0.65 and 100 pc. This interval is then sprinkled with random points of the same log D density as that of the real data.

The simulated points that lie on the log D axis are then projected onto a series of lines at different slopes (in steps of 0.1 from 1.5 to 4.5). Each of these lines passes through the extreme upper left-hand end of the best-fit line to the real data. We also added Gaussian noise in log Σ, which is related to the scatter of the real data by a parameter called "scatter." A scatter of 1 corresponds to the same standard deviation as that of the real data.

An appropriate sensitivity cutoff is applied to the simulated data points, selecting points above the sensitivity line (for

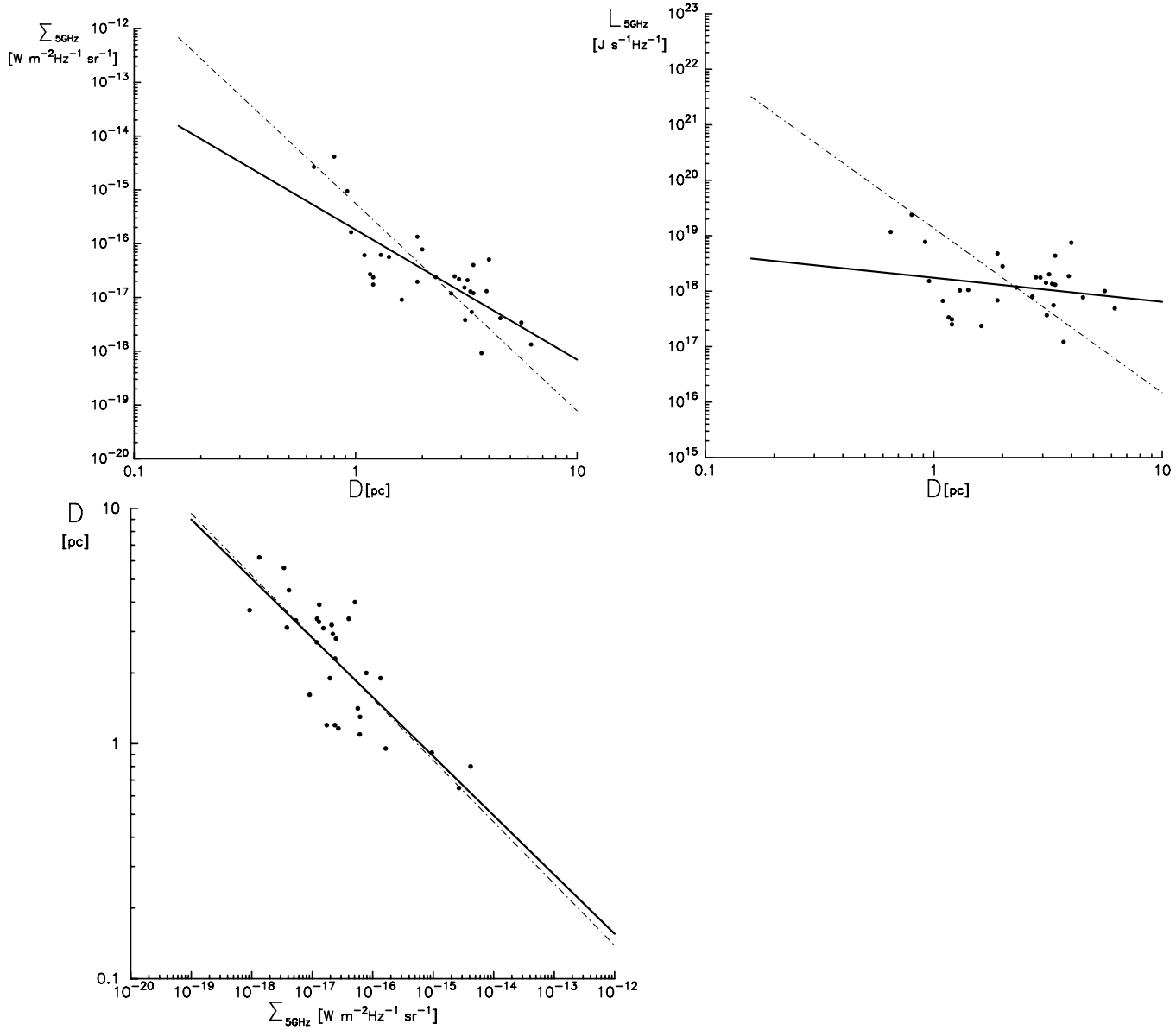

Figure 1. Data from Table 2 in F08 (31 SNRs). Thick solid line: non-weighted vertical offsets; dash-dotted line: non-weighted orthogonal offsets.

simplicity, we assumed a sensitivity line that passes through the real data point of the lowest brightness). This is done 1000 times for each simulated slope and a least-squares best-fit line (vertical regression) is generated for artificial samples.

In Table 5, the first column lists the scatter and the second column shows the value of the simulated slope. Columns 3–6 are for vertical offsets: the mean and standard deviation of the best-fit slopes for the generated samples and the mean and standard deviation of the best-fit slopes for sensitivity selected generated samples. In the same manner, Columns 7–10 list the properties for orthogonal offsets. Figure 3 shows one of our Monte Carlo generated samples for vertical offsets at 5 GHz with a scatter of 1 and the simulated slope of 2.4.

5.2. Orthogonal Offsets

We calculated the standard deviation of data from the data best-fit line using the orthogonal offsets. Then we have generated random diameters as described above. The points are then projected onto the simulated slope line. Then we added the Gaussian noise to the simulated points in the orthogonal direction from the simulated slope line as

$$D_{\rm noise} = D_{\rm proj} \pm \frac{n_{\rm orth.}}{\sqrt{1+\frac{1}{b^2}}}, \quad \Sigma_{\rm noise} = \Sigma_{\rm proj} \pm \frac{n_{\rm orth.}}{1+b^2}, \qquad (3)$$

with $n_{\rm orth.}$ being the noise in the orthogonal offset direction and b being the simulated slope. All artificial samples are fitted using orthogonal fitting procedure repeated 1000 times. The results of Monte Carlo simulations for orthogonal offsets are presented in Figure 3 (for slope $\beta = 3.9$) and Table 5.

6. DISCUSSION

By contrast to the standard (vertical) fitting, the orthogonal regression procedure leads to a significant change in the slope of the Σ–*D* relation from 2.4 to 3.9 (Table 2). The latter is a steep empirical slope, very far away from the trivial one ($\beta \approx 2$), and between theoretical predictions for the energy conserving phase of an SNR evolution ($\beta = 3.5$ and 4.25),

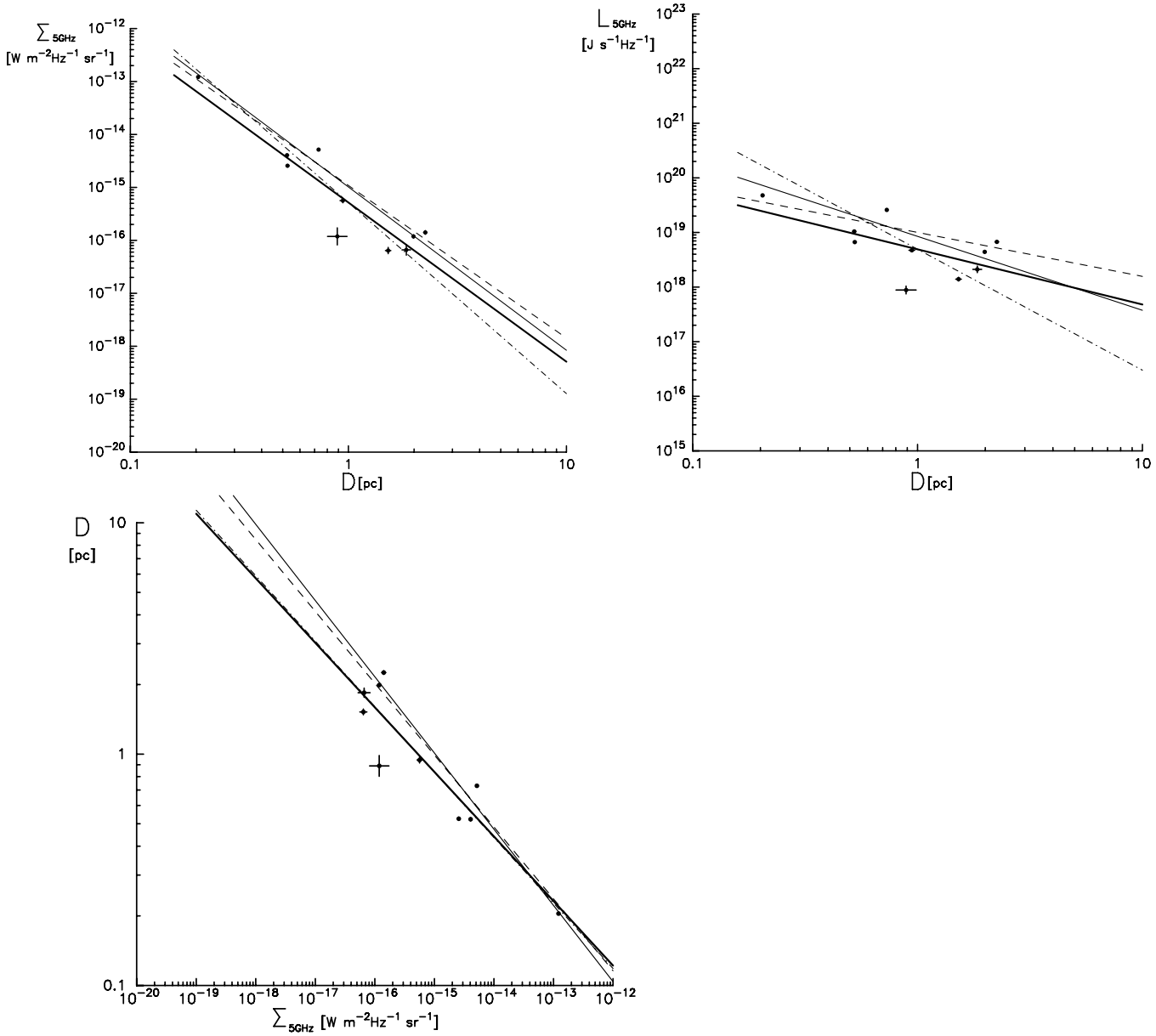

Figure 2. Data from Table 3 in F08 (10 SNRs). The errors are plotted for all points. Thick solid line: non-weighted vertical offsets; dashed line: weighted vertical offsets; the dash-dotted and thin solid lines are for the non-weighted and weighted orthogonal offsets, respectively.

obtained by Duric & Seaquist (1986) and Berezhko & Völk (2004), respectively. The inverted slope value ($1/3.9 \approx 0.26$) is approximately the same as the value obtained by D–Σ fitting. Thus, for the orthogonal fitting procedure, D–Σ and Σ–D fit parameter values are invariant within the estimated uncertainties (see Tables 2 and 4). A careful inspection of Table 4 leads to the conclusion that both fitting procedures provide similar D–Σ slopes. Therefore, in the case of M82 SNRs, instead of using the more complicated orthogonal regression method, one can find the D–Σ slope by the standard (vertical) fitting and after that invert it to find a valid Σ–D slope. This supports a suggestion to use the D–Σ relation given by Green (2009). This is possible because of the narrow span of diameters for M82 SNRs (1 order of magnitude) in comparison to the wide span of brightnesses (4 orders of magnitude). If these spans are similar, the orthogonal procedure has to be used for the useful D–Σ regression, too.

Based on the L–D analysis (Table 3), it can be concluded that corresponding correlations are very poor. A large scatter in the data is evident and hence the correlation coefficients are low. On the other hand, some poor trends in the L–D plane are visible but the moderately large level of scattering (or a small number of objects) in analyzed samples could not provide any valid conclusion about these trends (see Figures 1 and 2, second panel). There are observed differences in the expansion velocities of the SNRs in M82 (see F08, and references therein). This implies that they are either on different evolutionary tracks (connected with different initial energy of explosion), and/or expanding into different density regions, or as a consequence, may be in different phases of SNR evolution. Consequently, a relatively large data scatter can be explained by the above noted influences.

When presenting fit parameter values in the tables, we have given the ratio of weighted sum of square residuals (offsets) and number of degrees of freedom (WSSR/ndof). The probability Q of obtaining larger WSSRs is also presented. While for non-weighted offsets WSSR/ndof and Q values are of no

Table 5
Results of Monte Carlo Simulations

		Vertical offsets				Orthogonal offsets			
Scatter	Simulated Slope	Mean Simulated Slope	SD of Mean Simulated Slope	Mean Slope After Selection	SD of Slope After Selection	Mean Simulated Slope	SD of Mean Simulated Slope	Mean Slope After Selection	SD of Slope After Selection
1.0	1.500000	1.500696	0.099013	1.286365	0.109226	1.497463	0.055816	1.497168	0.055705
1.0	1.600000	1.600147	0.104393	1.349833	0.123326	1.598297	0.057974	1.587014	0.058188
1.0	1.700000	1.699489	0.099988	1.426584	0.131765	1.702749	0.060101	1.683068	0.067908
1.0	1.800000	1.802722	0.101126	1.507596	0.148833	1.804823	0.063576	1.782269	0.076331
1.0	1.900000	1.899529	0.101864	1.576387	0.156577	1.901645	0.065447	1.878356	0.082454
1.0	2.000000	1.997602	0.096299	1.672339	0.168350	2.003504	0.066718	1.979787	0.094530
1.0	2.100000	2.101995	0.101180	1.751897	0.183618	2.097585	0.069813	2.071091	0.112198
1.0	2.200000	2.203092	0.101992	1.836862	0.198541	2.201668	0.070944	2.182622	0.121677
1.0	2.300000	2.298177	0.100645	1.911342	0.212355	2.297719	0.078436	2.278483	0.139566
1.0	2.400000	2.402304	0.099143	2.005975	0.228506	2.402684	0.080858	2.384728	0.146849
1.0	2.500000	2.500295	0.100127	2.098402	0.243022	2.504435	0.081318	2.481287	0.165271
1.0	2.600000	2.602096	0.101548	2.172323	0.261917	2.600812	0.088288	2.576799	0.184526
1.0	2.700000	2.702694	0.101349	2.266196	0.287042	2.704265	0.085594	2.675869	0.204002
1.0	2.800000	2.799537	0.100410	2.340753	0.298422	2.799311	0.090789	2.784884	0.229936
1.0	2.900000	2.897140	0.098674	2.421775	0.310348	2.899872	0.095418	2.877078	0.238608
1.0	3.000000	2.996749	0.099588	2.498980	0.323027	3.003264	0.098458	2.979326	0.249424
1.0	3.100000	3.104522	0.098841	2.589717	0.345333	3.102771	0.102963	3.076613	0.290303
1.0	3.200000	3.202747	0.102624	2.688157	0.357554	3.204156	0.104733	3.179113	0.326909
1.0	3.300000	3.298963	0.099057	2.763613	0.362475	3.300337	0.106178	3.290091	0.310472
1.0	3.400000	3.402224	0.102481	2.839851	0.412462	3.405014	0.104106	3.377635	0.405915
1.0	3.500000	3.507588	0.104501	2.953550	0.443178	3.500932	0.107231	3.498262	0.398552
1.0	3.600000	3.601357	0.098950	3.027741	0.440752	3.603510	0.113465	3.603639	0.441060
1.0	3.700000	3.698463	0.102682	3.100663	0.431116	3.699302	0.115896	3.686992	0.517250
1.0	3.800000	3.800653	0.102899	3.198014	0.492386	3.809688	0.118302	3.789941	0.506556
1.0	3.900000	3.901953	0.100244	3.276876	0.484156	3.907993	0.121222	3.879406	0.624074
1.0	4.000000	3.997578	0.100347	3.371390	0.524299	4.003947	0.128336	3.956310	0.633162
1.0	4.100000	4.098606	0.103149	3.451102	0.567184	4.101723	0.127667	4.003518	0.836152
1.0	4.200000	4.203367	0.099424	3.549554	0.561571	4.205925	0.131813	4.103016	0.918963
1.0	4.300000	4.296356	0.103596	3.563594	0.564266	4.301982	0.133642	4.140517	0.947753
1.0	4.400000	4.399762	0.102086	3.677029	0.617068	4.396678	0.136565	4.231672	1.092972
1.0	4.500000	4.500762	0.099421	3.754998	0.640986	4.513678	0.138215	4.261958	1.206376
2.0	1.500000	1.497074	0.201499	1.010993	0.208958	1.503948	0.123884	1.491782	0.120576
2.0	1.600000	1.601748	0.206268	1.059087	0.211039	1.611962	0.125516	1.565151	0.122074
2.0	1.700000	1.699103	0.206710	1.097170	0.225302	1.709634	0.127692	1.629440	0.129925
2.0	1.800000	1.815947	0.198277	1.148707	0.227667	1.806221	0.136550	1.718790	0.151350
2.0	1.900000	1.898634	0.205865	1.184780	0.240272	1.906057	0.140358	1.818100	0.177176
2.0	2.000000	2.003181	0.208126	1.229978	0.239254	2.001608	0.141960	1.909523	0.193236
2.0	2.100000	2.106723	0.196232	1.282816	0.266664	2.115680	0.149275	2.012858	0.243819
2.0	2.200000	2.195067	0.200040	1.317523	0.278585	2.214054	0.154374	2.100802	0.277017
2.0	2.300000	2.297552	0.198016	1.378041	0.304825	2.310805	0.166987	2.184658	0.346117
2.0	2.400000	2.402734	0.192766	1.457052	0.326163	2.403606	0.169570	2.268059	0.405243
2.0	2.500000	2.500341	0.191161	1.510620	0.345794	2.519952	0.178789	2.328069	0.539537
2.0	2.600000	2.603374	0.201804	1.553823	0.358145	2.606837	0.179346	2.382969	0.617191
2.0	2.700000	2.696222	0.194625	1.628281	0.407107	2.702147	0.182631	2.305122	0.883883
2.0	2.800000	2.802244	0.198338	1.671113	0.416296	2.818203	0.190096	2.292552	0.999156
2.0	2.900000	2.904717	0.209044	1.757733	0.452250	2.918469	0.191426	2.191101	1.186119
2.0	3.000000	3.000119	0.200248	1.794150	0.449686	3.009131	0.205601	2.091009	1.306820
2.0	3.100000	3.095304	0.199938	1.861154	0.493821	3.120773	0.203151	2.027416	1.389508
2.0	3.200000	3.206066	0.200175	1.928786	0.495782	3.210318	0.209492	1.922314	1.469364
2.0	3.300000	3.305481	0.191043	2.017072	0.513027	3.318200	0.220698	1.704367	1.569541
2.0	3.400000	3.397078	0.198111	2.045195	0.562483	3.406487	0.224814	1.631980	1.610402
2.0	3.500000	3.510252	0.208732	2.105675	0.588506	3.516766	0.231254	1.439036	1.648696
2.0	3.600000	3.602030	0.206381	2.150111	0.604538	3.619306	0.233198	1.341696	1.673103
2.0	3.700000	3.691687	0.201116	2.245178	0.687834	3.713207	0.232729	1.240939	1.677783
2.0	3.800000	3.814261	0.194869	2.285464	0.694195	3.822946	0.250042	1.173427	1.684988
2.0	3.900000	3.899518	0.198059	2.332963	0.720083	3.915391	0.253124	1.115622	1.664230
2.0	4.000000	4.007378	0.208750	2.446729	0.717167	4.025399	0.257137	0.951611	1.650998
2.0	4.100000	4.108197	0.209448	2.473150	0.788030	4.117051	0.254371	0.863239	1.593827
2.0	4.200000	4.203942	0.206663	2.561313	0.789212	4.232547	0.274843	0.830775	1.621492
2.0	4.300000	4.303620	0.199229	2.637333	0.854930	4.325485	0.272846	0.783813	1.597587
2.0	4.400000	4.399662	0.196009	2.689233	0.854584	4.413641	0.279349	0.608025	1.497785
2.0	4.500000	4.515249	0.199041	2.720509	0.910855	4.513320	0.282582	0.701798	1.558721

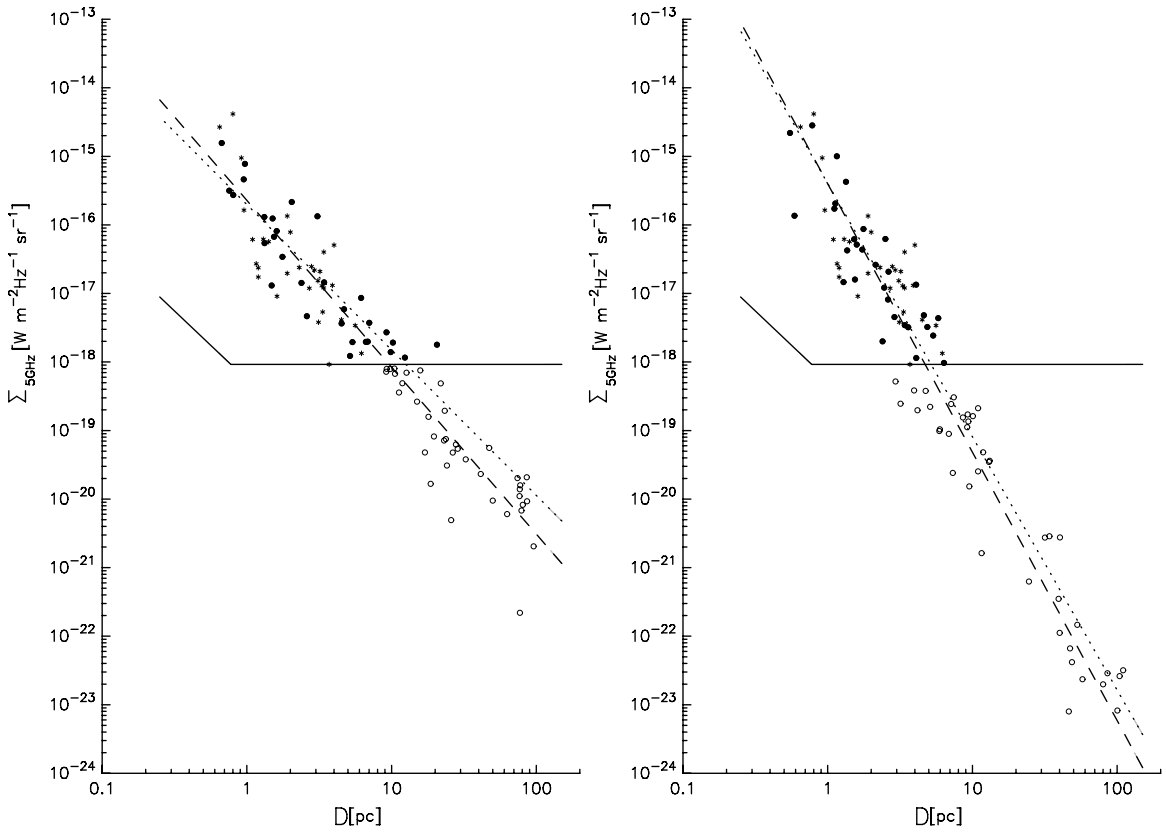

Figure 3. Monte Carlo generated sample at 5 GHz for a scatter of 1. M82 data points (31 SNRs, signed by asterisks) are plotted together with the sensitivity (solid) line; artificially generated points are plotted above (filled circles) and below (open circles) this line. Dashed line: fit before selection; dotted line: fit after selection. Left: vertical offsets for a simulated slope of 2.4; right: orthogonal offsets for a simulated slope of 3.9.

practical importance and are calculated only for the sake of completeness, they show that weighted fits are not statistically justified ($Q \gtrsim 0.001$ and WSSR/ndof $\sim$1, when the scatter is on the order of $\sim$1 standard deviation).

Arbutina & Urošević (2005) argued that SNRs of different types can be found along more or less parallel tracks in the Σ–D plane. The tracks are presumably defined by the density of the surrounding environment in which SNRs evolve.

Inspection of Table 5 shows that for scatters larger than 1, slopes of the Σ–D relation are seriously under the influence of the sensitivity cutoff. This implies that for a reliable calibration of the Σ–D relation, compact samples should be used (SNRs with similar initial properties evolving in similar environments). This criterion is probably satisfied for the M82 SNR sample consisting of young SNRs that evolve in the dense environment of the M82 starburst region. The latter conclusions may be valid if all SNRs have entered the energy conserving (Sedov) phase. The exact phase of evolution remains the main uncertainty for M82 SNRs. At least one compact SNR 43.3+59.2 has an exponent m, from the dynamical law $R \propto t^m$, $\geqslant$0.68 implying the free expansion (Beswick et al. 2006). Chevalier & Fransson (2001), on the other hand, argue that M82 SNRs may even be in the radiative phase.

For the simulated data scatter of 1, that should resemble the real scatter of the data, the slope of the Σ–D relation is not severely biased by the sensitivity cutoff. A similar conclusion is drawn from the Monte Carlo sensitivity related simulations in Paper I. They used the M82 data sample of Huang et al. (1994), collected with the Very Large Array, while the M82 sample analyzed in this work was recorded with the MERLIN measurements. This resulted in somewhat different sensitivity lines but nevertheless both studies came up with similar conclusions.

Monte Carlo simulations are carried out for the purpose of checking the completeness of the M82 SNR sample. Objects with low surface brightnesses cannot be detected because they are affected by the survey sensitivity selection effect. By simulating this effect, we tried to find out whether our sample (i.e., corresponding Σ–D slope) is representative for M82 SNR population or not. Inspection of Table 5, when scatter is generated by vertical offsets, shows that the sensitivity selection effect makes the observed Σ–D slopes shallower. The result is identical to the one obtained in Paper I. When scatter is generated by the orthogonal offsets, the sensitivity line does not cut a significant number of artificial objects located in the lower left part of the field. In the scatter 1 scenario, the sensitivity cutoff does not affect the Σ–D slope (see Table 5). A very interesting situation arises in the simulation of the orthogonal scatter 2 scenario. The Σ–D slopes are changed significantly. The lower left part of the artificial samples is cut by the sensitivity line when scatter is high (higher than the real one) and the slopes of relations become shallower. Based on the analysis of the results of the simulations presented (Table 5), we believe that the orthogonal scatter 1 scenario is more likely for two reasons: (1) the slope ($\beta = 3.9$) is obtained by the orthogonal procedure that gives the invariant Σ–D and D–Σ slopes and (2) scatter is generated by the orthogonal offsets and corresponds to the real scatter in the observed data set. We conclude that the sensitivity selection effect does not have a major impact on the Σ–D slope for M82 SNRs.

With D–Σ and Σ–D fit slopes being invariant within the estimated uncertainties in the orthogonal fitting procedure,

assuming a relatively complete sample, the $\Sigma \propto D^{-3.9}$ relation for M82 SNRs could potentially describe the evolution of young SNRs in the energy conserving phase of their evolution, and this relation might be useful for estimating distances to such SNRs. The problem that remains is the coupling of the evident data scattering in the F08 SNR sample and a small number of objects for which reliable statistics can be done. Another problem is that most of the sources do not show a significant flux density variation (Kronberg et al. 2000), implying a trivial physical relation $L_\nu \approx$ const. Some sources, like 41.30+59.6, show flux increase rather than decrease (F08). Therefore, the Σ–D relations obtained in this paper should be used with caution.

Finally, some compact radio objects in M82 may not be SNRs as proposed by Seaquist & Stanković (2007). They analyzed compact non-thermal radio objects and concluded that some of them are probably the so-called wind-driven bubbles (WDBs) due to the lack of observed time variability in most of the sources, implying ages greater than expected for SNRs. However, the recent detection of γ radiation from M82 (Abdo et al. 2010) confirms the standard opinion that radio objects in M82 are indeed SNRs. The strong shock waves of young SNRs are necessary for the efficient production of cosmic rays by the so-called diffuse shock acceleration (DSA) mechanism. The inverse Compton scattering of the background electromagnetic radiation by the cosmic-ray electrons (leptonic model) or a decay of neutral pions, mainly produced by cosmic-ray protons during the interaction with the gas (hadronic model), represents two basic mechanisms for the production of γ rays. WDBs probably do not represent proper sites for the production of γ rays, due to slower shock waves in comparison to shock waves of young SNRs.

7. CONCLUSIONS

We suggest that the orthogonal regression procedure be used for obtaining empirical Σ–D relations. In that case, the values of parameters obtained from the fitting of Σ–D and D–Σ relations are invariant within estimated uncertainties. Alternatively, if a data span in Σ covers more orders of magnitude than a data span in D, the fitting of the D–Σ relation with vertical offsets can give a β that resembles the slope fitted with either Σ–D or D–Σ orthogonal offsets. The steep Σ–D slope ($\beta = 3.9$) is obtained when fitting the orthogonal regression to the updated M82 SNR sample. The results of our Monte Carlo simulations suggest that this slope is probably free of the sensitivity selection effect. Moreover, it is closer to the updated theoretically derived slopes for the energy conserving phase of SNR evolution. The relation $\Sigma \propto D^{-3.9}$ could represent the average evolutionary track for SNRs in M82, and could potentially be used for estimating the distances of young SNRs expanding in dense environment. However, data scattering and, more importantly, a relatively small number of objects in the analyzed samples constrain the reliability of this relation. Due to this, the obtained Σ–D relations should be used with caution. More observations and better theoretical description are necessary for a deeper understanding of the radio evolution of these SNRs.

The authors thank Dragana Momić for reading the manuscript and the anonymous referee for valuable comments that improved the quality of this paper. This work is part of Projects No. 146003 and 146012 supported by the Ministry of Science and Environmental Protection of Serbia.

REFERENCES

Abdo, A. A., et al. 2010, ApJ, 709, L152
Arbutina, B., & Urošević, D. 2005, MNRAS, 360, 76
Arbutina, B., Urošević, D., Stanković, M., & Tešić, Lj. 2004, MNRAS, 350, 346
Bandiera, R., & Petruk, O. 2010, A&A, 509, A34
Berezhko, E. G., & Völk, H. J. 2004, A&A, 427, 525
Beswick, R. J., et al. 2006, MNRAS, 369, 1221
Case, G. L., & Bhattacharya, D. 1998, ApJ, 504, 761
Chevalier, R. A., & Fransson, C. 2001, ApJ, 558, L27
Chomiuk, L., & Wilcots, E. M. 2009, AJ, 137, 3869
Clark, D. H., & Caswell, J. L. 1976, MNRAS, 174, 267
Duric, N., & Seaquist, E. R. 1986, ApJ, 301, 308
Fenech, D., Beswick, R., Muxlow, T. W. B., Pedlar, A., & Argo, M. K. 2010, arXiv:1006.1504
Fenech, D. M., Muxlow, T. W. B., Beswick, R. J., Pedlar, A., & Argo, M. K. 2008, MNRAS, 391, 1384 (F08)
Green, D. A. 1984, MNRAS, 209, 449
Green, D. A. 2009, Bull. Astron. Soc. India, 37, 45
Guseinov, O. H., Ankay, A., Sezer, A., & Tagieva, S. O. 2003, Astron. Astrophys. Trans., 22, 273
Huang, Z. P., Thuan, T. X., Chevalier, R. A., Condon, J. J., & Yin, Q. F. 1994, ApJ, 424, 114
Kronberg, P. P., Sramek, R. A., Birk, G. T., Dufton, Q. W., Clarke, T. E., & Allen, M. L. 2000, ApJ, 535, 706
McDonald, A. R., Muxlow, T. W. B., Pedlar, A., Garrett, M. A., Wills, K. A., Garrington, S. T., Diamond, P. J., & Wilkinson, P. N. 2001, MNRAS, 322, 100
McDonald, A. R., Muxlow, T. W. B., Wills, K. A., Pedlar, A., & Beswick, R. J. 2002, MNRAS, 334, 912
Milne, D. K. 1970, Aust. J. Phys., 23, 425
Milne, D. K. 1979, Aust. J. Phys., 32, 83
Muxlow, T. W. B., Pedlar, A., Wilkinson, P. N., Axon, D. J., Sanders, E. M., & de Bruyn, A. G. 1994, MNRAS, 266, 455
O'Neil, R. 1971, J. R. Stat. Soc. C: Appl. Stat., 20, 338
Pedlar, A., Muxlow, T. W. B., Garrett, M. A., Diamond, P., Wills, K. A., Wilkinson, P. N., & Alef, W. 1999, MNRAS, 307, 761
Poveda, A., & Woltjer, L. 1968, AJ, 73, 65
Seaquist, E. R., & Stanković, M. 2007, ApJ, 659, 347
Urošević, D. 2002, Serb. Astron. J., 165, 27
Urošević, D., Pannuti, T. G., Duric, N., & Theodorou, A. 2005, A&A, 435, 437 (Paper I)
Xu, J.-W., Zhang, X.-Z., & Han, J.-L. 2005, Chin. J. Astron. Astrophys., 5, 165